Nuclear Physics B99 (1975) 1–12
© North-Holland Publishing Company

ELECTROPRODUCTION OF π^+ MESONS IN THE RESONANCE REGION

J.-C. ALDER *, H. BEHRENS **, F.W. BRASSE, W. FEHRENBACH ***,
J. GAYLER, S.P. GOEL ‡, R. HAIDAN, V. KORBEL ‡‡, J. MAY ‡‡
and M. MERKWITZ
Deutsches Elektronen-Synchroton DESY, Hamburg, Germany

Received 21 August 1975

Results on the reaction ep → $e'n\pi^+$ are presented in the mass range $1.355 \leqslant W \leqslant 1.775$ GeV at $q^2 = 1$ GeV^2 and in the range $1.415 \leqslant W \leqslant 1.595$ GeV at $q^2 = 0.6$ GeV^2. From the angular distribution of the π^+ meson the polarization terms $\sigma_u + \epsilon\sigma_L$, σ_p and σ_I have been determined in the range of production angles $0 < \theta^*_{\pi^+} \lesssim 63°$.

1. Introduction

We have reported recently on an experiment on η production in the resonance region [1]. Now we report on an analysis on the data of the reaction ep → $en\pi^+$ taken at the same experiment. Data on this channel are still rather scarce in the resonance region. The resonance structure observed by Evangelides et al. [2] at forward angles shows that there are resonant amplitudes with total helicity $\frac{1}{2}$ of the ingoing virtual photon and proton. Photoproduction on the other hand is known to be dominated by helicity $\frac{3}{2}$ resonance excitation. It is one of the big successes of the quark model to predict the main features of photoproduction in the resonance region, in particular the dominance of the helicity $\frac{3}{2}$ amplitudes. The structures observed at space-like four-momentum transfers can therefore be very useful to test the model more severely.

The observed angular distributions of Evangelides et al. [2] at the second resonance region do not allow to separate the polarization terms $\sigma_u + \epsilon\sigma_L$, σ_p and σ_I. The present experiment covers the second resonance region at $q^2 = 0.6$ GeV^2 and the second and third resonance region at $q^2 = 1$ GeV^2. The obtained angular distri-

---

Present addresses:
* Université de Lausanne.
** Schulbehörde Hamburg.
*** Babcock-Brown-Boveri, Mannheim.
‡ On leave from Kurukshetra University, Kurukshetra, India.
‡‡ CERN, Geneva.

REQUEST

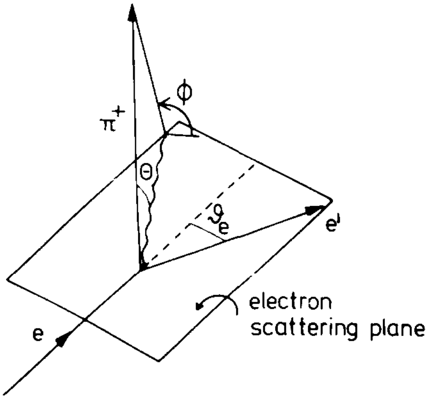

Fig. 1. Definition of angles.

butions have been analysed with respect to the polarization terms $\sigma_u + \epsilon\sigma_L$, σ_p and σ_I. First results of this experiment have been reported at the Bonn Conference 1973 [3].

2. Notation

We express the cross section in terms of the virtual photon absorption cross section $d\sigma/d\Omega^*_{\pi^+}$ in the c.m.s. of the final hadrons which is related to the differential coincidence cross section $d^5\sigma/dE'\,d\Omega_e\,d\Omega^*_{\pi^+}$ by the virtual photon flux factor Γ_t (defined as usually [4]):

$$\frac{d^5\sigma}{dE'\,d\Omega_e\,d\Omega^*_{\pi^+}} = \Gamma_t \frac{d\sigma}{d\Omega^*_{\pi^+}} . \tag{1}$$

The polar and azimuthal production angles (fig. 1) in the c.m.s. are denoted by θ^* and ϕ. The ϕ dependence of the angular distribution in the c.m.s. can be written [5] explicitly as

$$\frac{d\sigma}{d\Omega^*} = \sigma_u + \epsilon\sigma_L + \epsilon\cos 2\phi\,\sigma_p + \sqrt{2\epsilon(\epsilon+1)}\,\sigma_I\cos\phi . \tag{2}$$

The parameter ϵ describes the polarization of the virtual photon (e.g. ref. [4]). The cross sections σ_u, σ_L, σ_p and σ_I are functions of W, the invariant mass of the final $n\pi^+$ system, the momentum transfer q^2 and the angle θ^*. The terms σ_u and σ_L are the cross sections of unpolarized transverse and longitudinal virtual photons. They can only be separated by changing the polarization ϵ, not done here. σ_p takes account of the transverse polarization of the virtual photon and σ_I is a transverse-lon-

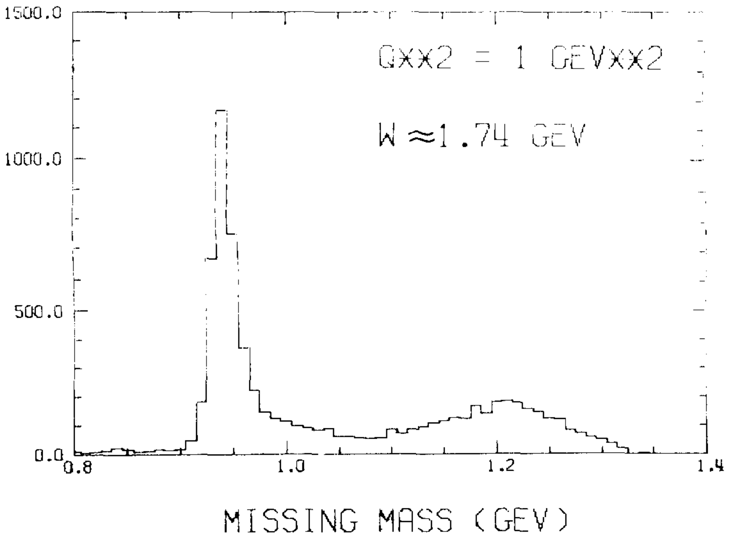

Fig. 2. Example of a missing mass distribution for π^+ detected in coincidence with electrons.

gitudinal interference term. A study of the ϕ dependence for fixed θ^* allows to separate the 3 terms $\sigma_u + \epsilon\sigma_L$, σ_p and σ_I.

3. Apparatus

The experimental setup is described in more detail in ref. [1]. Only a short description is repeated here. The measurements are done in an external e^- beam of DESY. The primary beam hits a 12 cm liquid hydrogen target. The intensity is controlled by a secondary emission monitor, which was compared many times during the experiment to a Faraday cup. The scattered electron is detected in a focussing vertically bending spectrometer. It is identified by a threshold CO_2 Čerenkov and a sandwich shower counter.

The π^+ meson is detected in coincidence with the scattered e^- in a non-focussing spectrometer consisting of a vertically bending magnet, a system of proportional chambers mounted at the magnet exit and a scintillator hodoscope. The trajectory is defined by the target and the intersections with the proportional chamber and the scintillator hodoscope.

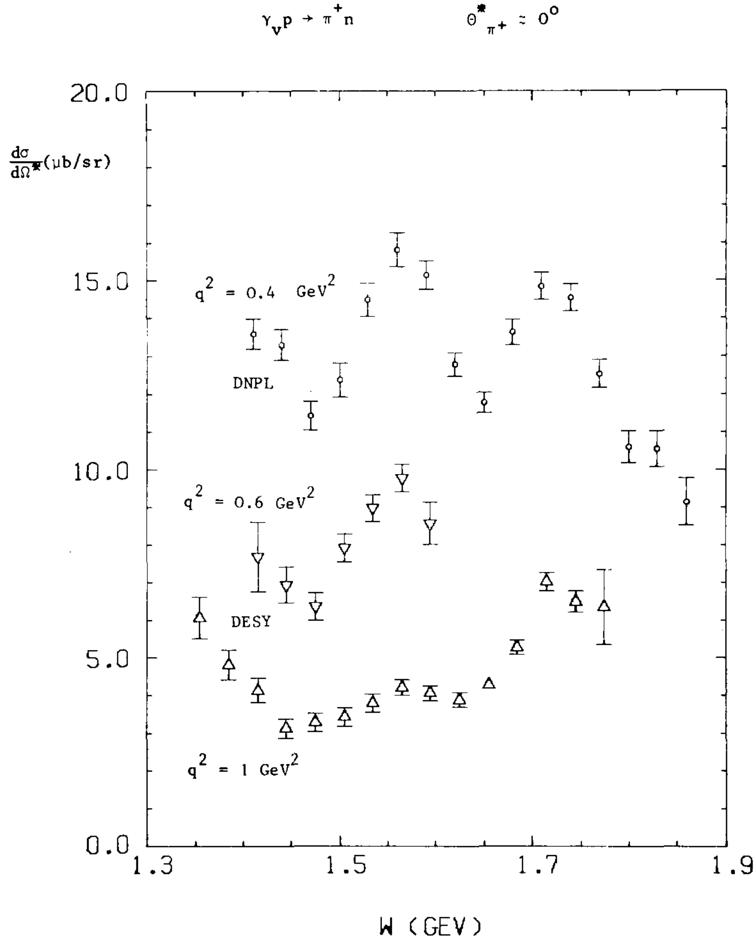

Fig. 3. Forward π^+ production cross section at $q^2 = 0.4$ from DNPL and at $q^2 = 0.6$ and 1 GeV^2 from DESY.

4. Data analysis

The π^+ mesons are distinguished from protons by time of flight [1]. The reaction ep → $e n \pi^+$ clearly shows up in the missing mass spectrum. An example is given in fig. 2. Events in the missing mass range 895 MeV to 1025 MeV have been used to calculate the cross sections of the reaction ep → $e\pi^+$n.

Acceptances and various corrections have been calculated by a Monte-Carlo simulation of the whole experiment. The W, q^2 and θ^* dependence of π^+ production

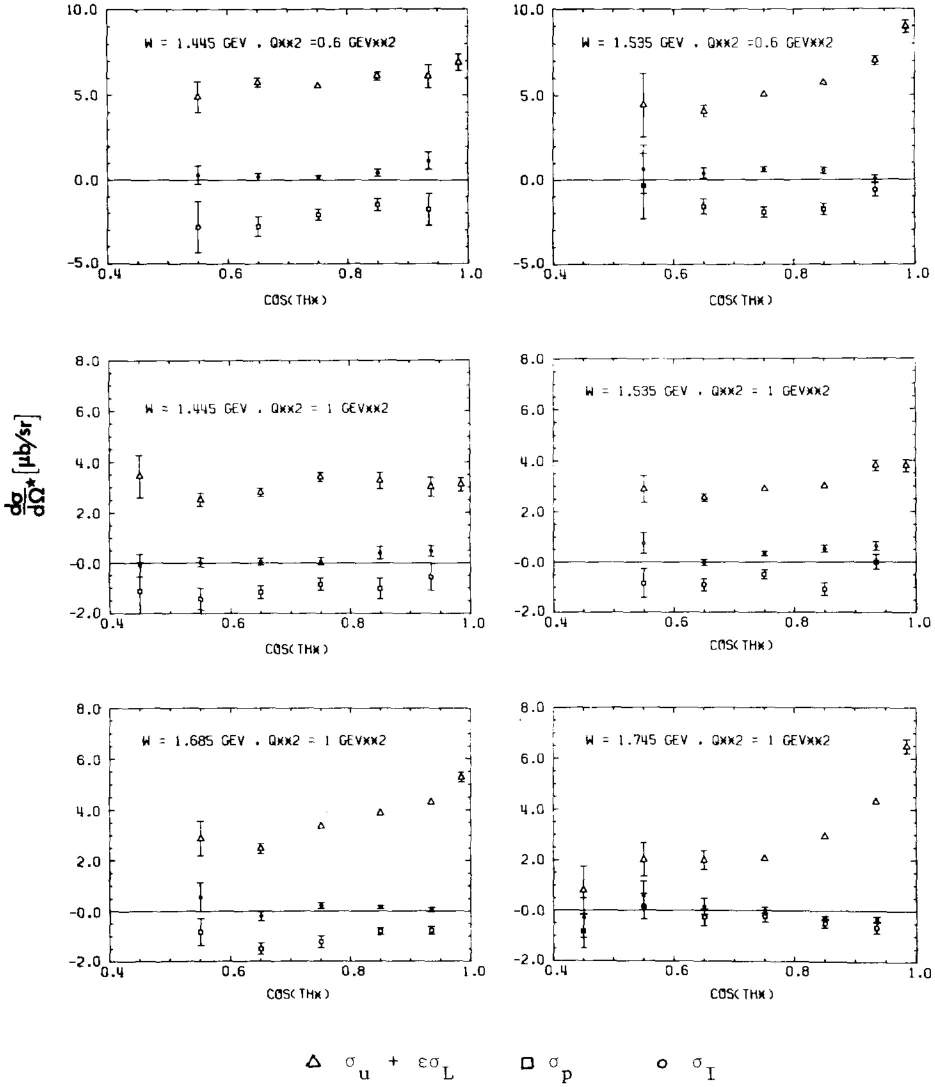

Fig. 4. Examples of angular distributions at $q^2 = 0.6$ and 1 GeV^2.

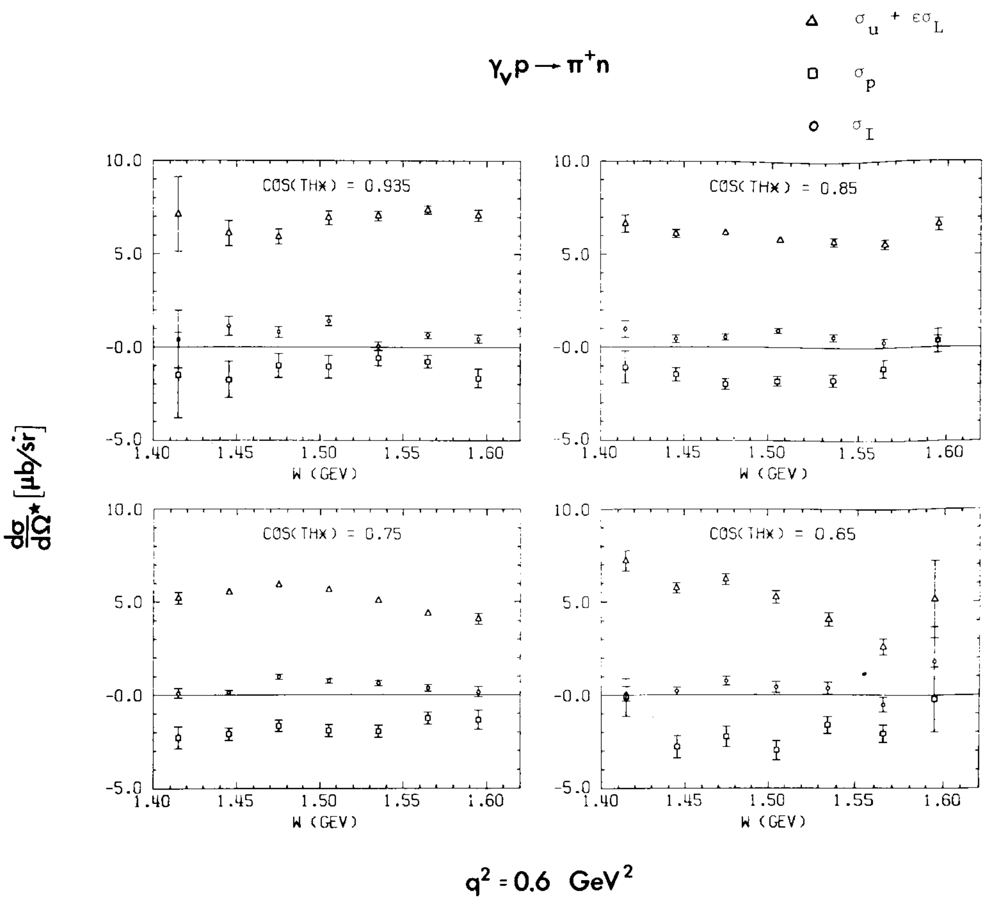

Fig. 5. $\sigma_u + \epsilon\sigma_L$ (△), σ_p (□) and σ_I (○) at different values of $\cos\theta^*$ as a function of W at $q^2 = 0.6$ GeV^2.

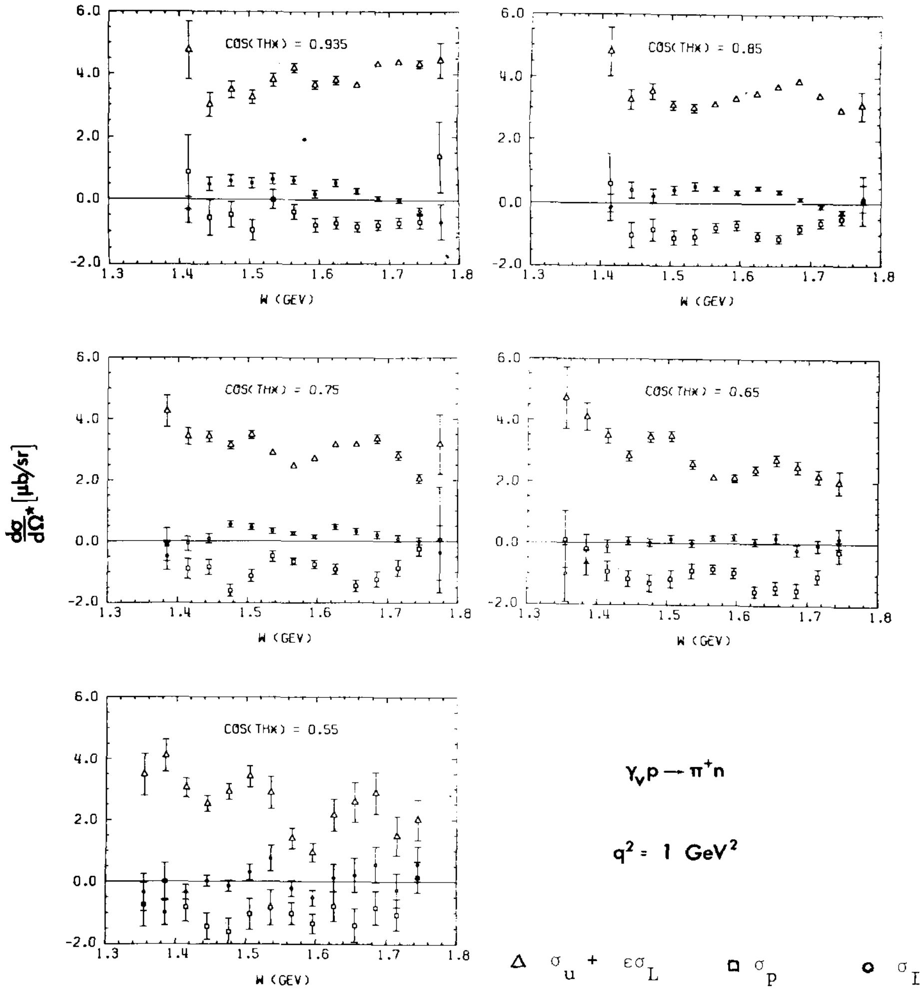

Fig. 6. $\sigma_u + \epsilon\sigma_L$ ($\triangle$), σ_p ($\square$) and σ_I ($\circ$) at different values of $\cos\theta^*$ as a function of W at $q^2 = 1$ GeV^2.

used for the simulation was taken from a preliminary analysis of a part of the data [3,6]. Also radiative corrections have been incorporated into the simulation including internal and external radiation. In this simulation only the radiation of the electron has been taken into account according to the formulas of ref. [7]. Radiation of the hadrons was taken account of in a second step: the ratio of radiative corrections with and without hadronic radiation was computed analytically according to

Table 1
Angular distributions of the reaction $\gamma_V p \to \pi^+ n$ (the errors do not contain an overall systematic error of 6%)

$\cos\theta^*$	$\sigma_u + \epsilon\sigma_L$ (μb/sr)	σ_P (μb/sr)	σ_I (μb/sr)
	W = 1.355 GeV	ϵ = 0.93	q^2 = 1.05 GeV^2
0.985	6.06 +- 0.56		
0.650	4.70 +- 1.00	0.11 +- 0.92	-1.00 +- 0.91
0.550	3.48 +- 0.69	-0.75 +- 0.70	-0.35 +- 0.60
	W = 1.385 GeV	ϵ = 0.93	q^2 = 1.04 GeV^2
0.985	4.80 +- 0.40		
0.750	4.26 +- 0.51	-0.11 +- 0.53	-0.49 +- 0.45
0.650	4.09 +- 0.45	-0.21 +- 0.47	-0.64 +- 0.41
0.550	4.10 +- 0.53	-0.00 +- 0.62	-0.99 +- 0.42
0.450	3.99 +- 0.80	0.25 +- 1.02	-0.94 +- 0.54
	W = 1.415 GeV	ϵ = 0.93	q^2 = 1.03 GeV^2
0.985	4.13 +- 0.32		
0.935	4.75 +- 0.94	0.86 +- 1.18	-0.33 +- 0.41
0.850	4.80 +- 0.77	0.63 +- 0.91	-0.13 +- 0.42
0.750	3.43 +- 0.27	-0.90 +- 0.32	-0.08 +- 0.24
0.650	3.48 +- 0.24	-0.93 +- 0.32	-0.13 +- 0.21
0.550	3.05 +- 0.31	-0.83 +- 0.46	-0.35 +- 0.23
	W = 1.445 GeV	ϵ = 0.92	q^2 = 1.02 GeV^2
0.985	3.11 +- 0.26		
0.935	3.01 +- 0.37	-0.56 +- 0.54	0.49 +- 0.22
0.850	3.27 +- 0.32	-1.02 +- 0.40	0.42 +- 0.25
0.750	3.42 +- 0.18	-0.84 +- 0.24	0.09 +- 0.16
0.650	2.82 +- 0.17	-1.16 +- 0.26	0.06 +- 0.14
0.550	2.52 +- 0.26	-1.44 +- 0.42	0.02 +- 0.18
0.450	3.45 +- 0.84	-1.12 +- 1.15	-0.09 +- 0.45
	W = 1.475 GeV	ϵ = 0.92	q^2 = 1.01 GeV^2
0.985	3.28 +- 0.25		
0.935	3.49 +- 0.26	-0.47 +- 0.39	0.60 +- 0.18
0.850	3.55 +- 0.25	-0.84 +- 0.35	0.25 +- 0.22
0.750	3.15 +- 0.13	-1.60 +- 0.20	0.56 +- 0.11
0.650	3.45 +- 0.16	-1.29 +- 0.27	0.02 +- 0.13
0.550	2.91 +- 0.26	-1.61 +- 0.44	-0.15 +- 0.19
	W = 1.505 GeV	ϵ = 0.92	q^2 = 0.99 GeV^2
0.985	3.42 +- 0.25		
0.935	3.25 +- 0.21	-0.94 +- 0.31	0.53 +- 0.16
0.850	3.10 +- 0.15	-1.10 +- 0.23	0.43 +- 0.13
0.750	3.48 +- 0.12	-1.12 +- 0.19	0.47 +- 0.10
0.650	3.48 +- 0.17	-1.16 +- 0.28	0.13 +- 0.13
0.550	3.41 +- 0.35	-1.04 +- 0.49	0.31 +- 0.25
	W = 1.535 GeV	ϵ = 0.91	q^2 = 0.98 GeV^2
0.985	3.79 +- 0.24		
0.935	3.80 +- 0.21	0.01 +- 0.30	0.65 +- 0.17
0.850	3.00 +- 0.13	-1.07 +- 0.25	0.55 +- 0.14

Table 1 (continued)

$\cos\theta^*$	$\sigma_u + \epsilon\sigma_L$ (μb/sr)	σ_p (μb/sr)	σ_I (μb/sr)
	W = 1.535 GeV	ϵ = 0.91	q^2 = 0.98 GeV^2
0.750	2.89 +- 0.11	−0.49 +- 0.18	0.34 +- 0.09
0.650	2.56 +- 0.15	−0.89 +- 0.24	−0.00 +- 0.12
0.550	2.88 +- 0.52	−0.84 +- 0.57	0.76 +- 0.41
	W = 1.565 GeV	ϵ = 0.91	q^2 = 0.97 GeV^2
0.985	4.20 +- 0.20		
0.935	4.18 +- 0.15	−0.37 +- 0.22	0.62 +- 0.13
0.850	3.13 +- 0.08	−0.78 +- 0.15	0.49 +- 0.07
0.750	2.46 +- 0.07	−0.66 +- 0.11	0.27 +- 0.06
0.650	2.13 +- 0.10	−0.83 +- 0.15	0.17 +- 0.09
0.550	1.40 +- 0.33	−1.02 +- 0.36	−0.22 +- 0.27
0.450	1.98 +- 0.81	−0.27 +- 0.52	0.57 +- 0.66
	W = 1.595 GeV	ϵ = 0.90	q^2 = 0.95 GeV^2
0.985	4.05 +- 0.20		
0.935	3.65 +- 0.13	−0.78 +- 0.22	0.18 +- 0.12
0.850	3.30 +- 0.08	−0.71 +- 0.15	0.35 +- 0.07
0.750	2.69 +- 0.08	−0.76 +- 0.13	0.16 +- 0.06
0.650	2.12 +- 0.12	−0.95 +- 0.16	0.20 +- 0.11
0.550	0.94 +- 0.30	−1.35 +- 0.31	−0.53 +- 0.25
0.450	1.43 +- 0.57	−0.88 +- 0.39	0.01 +- 0.47
	W = 1.625 GeV	ϵ = 0.90	q^2 = 0.94 GeV^2
0.985	3.87 +- 0.19		
0.935	3.79 +- 0.13	−0.71 +- 0.19	0.53 +- 0.11
0.850	3.47 +- 0.08	−1.04 +- 0.15	0.50 +- 0.06
0.750	3.16 +- 0.10	−0.90 +- 0.17	0.47 +- 0.09
0.650	2.38 +- 0.14	−1.55 +- 0.18	0.05 +- 0.13
0.550	2.15 +- 0.53	−0.80 +- 0.47	0.13 +- 0.44
0.450	1.46 +- 0.67	−1.14 +- 0.54	−0.28 +- 0.56
	W = 1.655 GeV	ϵ = 0.90	q^2 = 0.93 GeV^2
0.985	4.26 +- 0.18		
0.935	3.64 +- 0.11	−0.83 +- 0.15	0.28 +- 0.08
0.850	3.70 +- 0.08	−1.13 +- 0.14	0.39 +- 0.06
0.750	3.15 +- 0.11	−1.45 +- 0.18	0.32 +- 0.09
0.650	2.71 +- 0.17	−1.42 +- 0.20	0.18 +- 0.16
0.550	2.58 +- 0.65	−1.40 +- 0.53	0.21 +- 0.56
0.450	0.17 +- 0.92	−2.32 +- 0.73	−1.55 +- 0.76
	W = 1.685 GeV	ϵ = 0.89	q^2 = 0.91 GeV^2
0.985	5.26 +- 0.19		
0.935	4.32 +- 0.11	−0.76 +- 0.16	0.06 +- 0.08
0.850	3.87 +- 0.08	−0.82 +- 0.14	0.15 +- 0.06
0.750	3.36 +- 0.14	−1.22 +- 0.24	0.22 +- 0.11
0.650	2.47 +- 0.20	−1.50 +- 0.23	−0.22 +- 0.18
0.550	2.88 +- 0.68	−0.84 +- 0.53	0.56 +- 0.58
	W = 1.715 GeV	ϵ = 0.88	q^2 = 0.90 GeV^2
0.985	7.01 +- 0.24		
0.935	4.38 +- 0.11	−0.69 +- 0.17	0.00 +- 0.08
0.850	3.39 +- 0.08	−0.65 +- 0.14	−0.12 +- 0.06

Table 1 (continued)

$\cos\theta^*$	$\sigma_u + \epsilon\sigma_L$ (μb/sr)	σ_p (μb/sr)	σ_I (μb/sr)
	$W = 1.715$ GeV	$\epsilon = 0.88$	$q^2 = 0.90$ GeV^2
0.750	2.80 +- 0.14	−0.86 +- 0.26	0.09 +- 0.11
0.650	2.17 +- 0.22	−1.06 +- 0.23	−0.07 +- 0.19
0.550	1.48 +- 0.63	−1.06 +- 0.50	−0.27 +- 0.55
0.450	1.06 +- 0.95	−0.99 +- 0.71	−0.35 +- 0.79
	$W = 1.745$ GeV	$\epsilon = 0.88$	$q^2 = 0.88$ GeV^2
0.985	6.49 +- 0.27		
0.935	4.32 +- 0.13	−0.67 +- 0.21	−0.32 +- 0.10
0.850	2.93 +- 0.09	−0.50 +- 0.17	−0.28 +- 0.08
0.750	2.05 +- 0.14	−0.24 +- 0.23	0.01 +- 0.12
0.650	1.99 +- 0.37	−0.27 +- 0.33	0.17 +- 0.32
0.550	2.00 +- 0.65	0.16 +- 0.51	0.58 +- 0.57
0.450	0.81 +- 0.94	−0.82 +- 0.66	−0.29 +- 0.79
	$W = 1.775$ GeV	$\epsilon = 0.87$	$q^2 = 0.87$ GeV^2
0.985	6.34 +- 0.99		
0.935	4.43 +- 0.56	1.38 +- 1.12	−0.67 +- 0.55
0.850	3.08 +- 0.45	0.10 +- 0.79	0.17 +- 0.43
0.750	3.18 +- 0.97	0.06 +- 1.70	−0.37 +- 0.89
	$W = 1.415$ GeV	$\epsilon = 0.92$	$q^2 = 0.63$ GeV^2
0.985	7.68 +- 0.92		
0.935	7.13 +- 2.00	−1.50 +- 2.30	0.42 +- 1.55
0.850	6.66 +- 0.47	−1.09 +- 0.86	0.98 +- 0.46
0.750	5.20 +- 0.32	−2.28 +- 0.59	0.10 +- 0.27
0.650	7.21 +- 0.56	−0.12 +- 1.02	0.07 +- 0.40
	$W = 1.445$ GeV	$\epsilon = 0.92$	$q^2 = 0.62$ GeV^2
0.985	6.93 +- 0.48		
0.935	6.11 +- 0.68	−1.76 +- 0.96	1.14 +- 0.50
0.850	6.12 +- 0.23	−1.47 +- 0.36	0.45 +- 0.20
0.750	5.51 +- 0.17	−2.09 +- 0.33	0.13 +- 0.13
0.650	5.75 +- 0.27	−2.78 +- 0.59	0.22 +- 0.21
0.550	4.89 +- 0.90	−2.82 +- 1.52	0.29 +- 0.55
	$W = 1.475$ GeV	$\epsilon = 0.91$	$q^2 = 0.61$ GeV^2
0.985	6.36 +- 0.37		
0.935	5.91 +- 0.41	−1.00 +- 0.64	0.81 +- 0.29
0.850	6.17 +- 0.20	−1.99 +- 0.30	0.55 +- 0.16
0.750	5.91 +- 0.16	−1.66 +- 0.31	0.97 +- 0.13
0.650	6.22 +- 0.30	−2.25 +- 0.55	0.77 +- 0.24
0.550	8.49 +- 2.55	2.01 +- 3.13	2.14 +- 1.63
	$W = 1.505$ GeV	$\epsilon = 0.91$	$q^2 = 0.60$ GeV^2
0.985	7.91 +- 0.37		
0.935	6.95 +- 0.37	−1.07 +- 0.61	1.42 +- 0.27
0.850	5.82 +- 0.18	−1.83 +- 0.26	0.90 +- 0.14
0.750	5.64 +- 0.16	−1.92 +- 0.31	0.75 +- 0.14
0.650	5.26 +- 0.34	−2.98 +- 0.52	0.43 +- 0.30
0.550	6.60 +- 2.23	−0.16 +- 2.59	1.03 +- 1.59

Table 1 (continued)

$\cos\theta^*$	$\sigma_u + \epsilon\sigma_L$ (μb/sr)	σ_p (μb/sr)	σ_I (μb/sr)
	$W = 1.535$ GeV	$\epsilon = 0.90$	$q^2 = 0.59$ GeV^2
0.985	8.97 +- 0.36		
0.935	7.05 +- 0.26	−0.60 +- 0.40	0.06 +- 0.22
0.850	5.74 +- 0.22	−1.77 +- 0.35	0.55 +- 0.19
0.750	5.07 +- 0.17	−1.96 +- 0.31	0.63 +- 0.15
0.650	4.06 +- 0.36	−1.63 +- 0.46	0.38 +- 0.32
0.550	4.44 +- 1.88	−0.36 +- 1.94	0.64 +- 1.45
	$W = 1.565$ GeV	$\epsilon = 0.90$	$q^2 = 0.58$ GeV^2
0.985	9.77 +- 0.37		
0.935	7.38 +- 0.22	−0.78 +- 0.35	0.66 +- 0.18
0.850	5.56 +- 0.26	−1.13 +- 0.46	0.26 +- 0.23
0.750	4.37 +- 0.18	−1.26 +- 0.31	0.38 +- 0.17
0.650	2.60 +- 0.43	−2.09 +- 0.48	−0.53 +- 0.40
	$W = 1.595$ GeV	$\epsilon = 0.89$	$q^2 = 0.57$ GeV^2
0.985	8.57 +- 0.56		
0.935	7.08 +- 0.29	−1.68 +- 0.49	0.46 +- 0.22
0.850	6.60 +- 0.35	0.34 +- 0.65	0.35 +- 0.29
0.750	4.08 +- 0.30	−1.34 +- 0.51	0.17 +- 0.29
0.650	5.15 +- 2.08	−0.23 +- 1.75	1.82 +- 1.86

the formulas of Bartl and Urban [8]. This latter correction was smaller than 2% in the covered kinematic range. Pion decay and subsequent tracing of the decay muon has also been included into the Monte-Carlo calculation. The resulting corrections were smaller than 4%.

The cross sections are corrected for empty target rate ($\simeq$0.5%), nuclear absorption ($\simeq$1%), dead time losses, inefficiencies, multi track events and random background.

5. Results

All data have been taken with the central electron spectrometer angle set to 15°. The polarization parameter ϵ was always close to 0.9. The errors given in the figures are statistical only. An overall systematic error of 6% should be taken into account.

The measured angular distributions cover a range from $\theta^*_{\pi^+} = 0^\circ$ up to nearly 90°. However, only in the range $0 \leqslant \theta^*_{\pi^+} \leqslant 65^\circ$ a sufficient range of ϕ angles was covered to separate the terms $\sigma_u + \epsilon\sigma_L$, σ_p and σ_I. These terms have been determined by least squares fits of all differential cross sections at fixed W, q^2 and $\cos\theta^*$ to the ϕ dependence of eq. (2). The results are given in table 1 and figs. 4 to 6. The cross sections $\sigma_u + \epsilon\sigma_L$ at $\cos\theta^* = 0.985$ have been obtained by averaging over all events of a given W, q^2 bin with $\cos\theta^* > 0.97$. The full table of differential cross sections is given in ref. [10].

The results on the forward cross sections confirm the structure observed by Evangelides et al. [2] at smaller momentum transfer (fig. 3), indicating that there are resonant helicity $\frac{1}{2}$ amplitudes. The cross section increases at $W \gtrsim 1.65$ GeV at $q^2 = 1$ GeV^2 even more than at $q^2 = 0.4$ GeV^2. This structure in W is nearly absent slightly off the forward direction at $\cos\theta^* = 0.935$ (fig. 6). The typical resonance structure of the second and third resonance region develops then more and more distinctly as the pions are produced more off the forward direction. We conclude that the helicity $\frac{3}{2}$ amplitudes contribute still considerably to the resonances at momentum transfers up to 1 GeV^2. The longitudinal-transverse interference term σ_I is rather small everywhere, at $W \approx 1700$ MeV it is essentially zero.

The smallness of σ_I was predicted in a recent extensive multipole analysis of pion production in the resonance region by Devenish and Lyth [9]. In this analysis preliminary data of the present experiment only at ϕ angles close to 90° have been used. The sharp rise observed above $W = 1.65$ GeV in the forward cross section is expected to be mainly due to σ_L from pion exchange.

The excellent performance of the Synchroton crew, the Hallendienst and the Rechenzentrum is gratefully acknowledged. We appreciate the technical assistance of J. Koll, G. Singer, K. Thiele, H. Weiss and Mrs. K. Schmöger. We thank E. Gaussauge for his help in the early stage of the experiment. Discussions with R.C.E. Devenish and F. Gutbrod are gratefully acknowledged.

References

[1] J.-C. Alder, F.W. Brasse, W. Fehrenbach, J. Gayler, R. Haidan, G. Gloe, S.P. Goel, V. Korbel, W. Krechlok, J. May, M. Merkwitz, R. Schmitz and W. Wagner, Nucl. Phys. B91 (1975) 386.
[2] E. Evangelides, R. Meaburn, J. Allison, B. Dickinson, M. Ibbotson, R. Lawson, H.E. Montgomery, D. Baxter, F. Foster, G. Hughes, P.S. Kummer, D.H. Lyth, R. Siddle and R.C.E. Devenish, Nucl. Phys. B71 (1974) 381.
[3] J.-C. Alder et al., Contribution to the 6th Int. Symp. on electron and photon interactions at high energies, Bonn 1973;
A.B. Clegg, Proc. 6th Int. Symp. on electron and photon interactions at high energies, Bonn, 1973 (North-Holland, Amsterdam, 1974).
[4] J.-C. Alder et al., Nucl. Phys. B46 (1972) 573.
[5] K. Berkelman, Proc. Int. Symp. on electron and photon interactions at high energies, Hamburg, 1965;
M. Gourdin, Nuovo Cimento 21 (1961) 1094.
[6] H. Behrens, Diplomarbeit, Universität Hamburg (1974).
[7] G. Miller, Thesis, Stanford University (1971).
[8] A. Bartl and P. Urban, Acta Phys. Austriaca 24 (1966) 139;
P. Urban, Topics in applied QED (Springer, Wien-New York, 1970).
[9] R.C.E. Devenish and D.H. Lyth, Nucl. Phys. B93 (1975) 109.
[10] J.-C. Alder et al., DESY 75/29 (1975).